

Phase diagrams of dilute Ising antiferromagnets

This article has been downloaded from IOPscience. Please scroll down to see the full text article.

1989 J. Phys.: Condens. Matter 1 5473

(<http://iopscience.iop.org/0953-8984/1/32/016>)

View [the table of contents for this issue](#), or go to the [journal homepage](#) for more

Download details:

IP Address: 171.66.16.93

The article was downloaded on 10/05/2010 at 18:36

Please note that [terms and conditions apply](#).

Phase diagrams of dilute Ising antiferromagnets

Serge Galam[†], P Azaria[‡] and H T Diep^{§||}

[†] Département de Recherches Physiques, T22-E3, Université Pierre et Marie Curie, 75252 Paris Cédex 05, France

[‡] Laboratoire de Magnétisme des Surfaces, Université Paris 7, 75251 Paris Cédex 05, France

[§] Fundamental Research Laboratories, NEC Corporation 4-1-1 Miyazaki, Miyamae-ku, Kawasaki 213, Japan

Received 6 October 1988

Abstract. Using the Monte Carlo technique the phase diagram of dilute Ising antiferromagnets in a field is found to be non-universal. Depending on the values of both the dilution and ratio of next-nearest- to nearest-neighbour interactions, the transition from the disordered phase as a function of the field can either be always continuous, or first order with a tricritical point. A new probabilistic mean-field theory which reproduces the qualitative features of Monte Carlo simulations is also presented. Experimental results are thus expected to depend on the nature of the specific materials used.

1. Introduction

The random field Ising model (RFIM) has been quite challenging for both theorists and experimentalists over the last decade. After a long period of controversy, the existence of long range order in three dimensions has been established by a rigorous work [1] thus confirming an earlier domain-wall argument [2] in favour of a lower critical dimension $d_1 = 2$.

The nature of the global phase diagram associated to three-dimensional random field systems is not yet well understood. Monte Carlo (MC) results of the $d = 3$ RFIM with a bimodal distribution were interpreted in support of a first-order transition even at very low fields [3], thus excluding a tricritical point, in contrast with mean field results [4]. Nevertheless, these MC results [3] have been also discussed as being consistent with a continuous transition, providing dynamical effects are included [5].

Experimentally, random fields are obtained by applying a uniform field on dilute antiferromagnets [6]. Substitutional site disorder is the most usual experimental situation [7]. However, the rapid increase of the equilibrium time when the transition is approached from above makes it difficult to achieve equilibrium experimentally [8]. These difficulties have been explained by the formation of domains and pinning in the RFIM [9].

In parallel, MC simulations of a three-dimensional dilute Ising antiferromagnet with nearest-neighbour (NN) interactions in a field [10] suggested a continuous transition even for strong fields at a concentration $p = 0.3$ of non-magnetic sites. In contrast, recent MC

|| On leave from Laboratoire de Magnétisme des Surfaces, Université Paris 7, 75251 Paris Cédex 05, France.

studies of the same model at a concentration $p = 0.2$ found a tricritical point by including next-nearest-neighbour (NNN) interactions for a ratio $\alpha = -0.5$ of NNN to NN interactions [11].

In this paper we present for the first time a systematic investigation of the phase diagram of dilute Ising antiferromagnets in a uniform field as function of both dilution and ratio of NNN to NN interactions on a cubic lattice. The inclusion of both NN and NNN makes the model closer to experimental random-field systems. The order of the transition from the disordered phase is found to be non-universal: the phase diagram depends strongly on the values of p and α . We find a tricritical point in the range of dilution $0 \leq p \leq 0.3$ for a ratio $\alpha = -0.5$. The tricritical point moves towards lower temperatures and weaker fields with increasing p , thus making the first-order region shrink. On the other hand, we show that increasing α enlarges the first-order region. To discuss these results we present a new probabilistic treatment which yields the correct qualitative features of the phase diagram. This approach justifies qualitatively a recent prediction [12] of a tricritical point with a p -dependence for dilute Ising systems.

2. Monte Carlo results

We consider the following Hamiltonian

$$\mathcal{H} = J \sum_{\langle i,j \rangle} S_i S_j + \alpha J \sum_{\langle i,k \rangle} S_i S_k - H \sum_i S_i, \quad (1)$$

where $J > 0$ is taken as unit of energy, α is the ratio of NNN to NN and H is the applied uniform magnetic field. The Ising spins S_i take the values ± 1 except at a concentration p of lattice sites where they are zero. These vacant sites are chosen at random. The first two sums in equation (1) are performed over all NN and NNN pairs, respectively, while the last sum is performed over all occupied lattice sites.

We have carried out extensive MC simulations with different simple cubic lattice samples of size $N = 20^3$. Finite size effects have been studied for one case ($p = 0.2$, $\alpha = -0.5$) [11]. The periodic boundary conditions have been imposed throughout. The MC technique used here is the single-spin flipping procedure where in each run we discard a sufficient number of MC steps (MCS) per spin to equilibrate the system before averaging physical quantities over a number of MCS/spin. The two following procedures have been used in our simulations: (i) applying H on the antiferromagnetic (AF) and ferromagnetic (F) initial spin configurations at a given temperature T ; (ii) heating or cooling the system at a given field H . The choice of the former or the latter procedure depends on the trajectory followed in the simulation with respect to the critical line in the TH plane. The first procedure is convenient at high values of H while the second one is more suitable at low values of H . The use of AF and F configurations as initial conditions helps to stabilise the system more rapidly than the use of random initial configurations. The AF is one of the ground states of the system when H does not exceed the critical value $H_c(p)$ given by $H_c(p) = (1 - p)H_0$ where $H_0 = 6$ for simple cubic structures. The F state on the other hand is the stable configuration at high temperatures in a non-zero field. In addition, at each concentration p we used different samples to make sure that the results are independent of vacant site distributions. In some cases (large values of p), up to 10 samples have been used.

In order to determine the nature of the phase transition we detect the hysteresis upon applying H with AF and F initial spin configurations or upon heating and cooling the

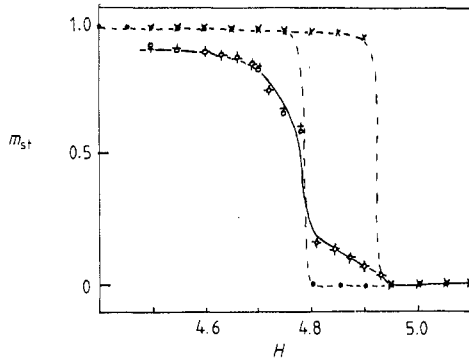


Figure 1. Staggered magnetisation m_{st} versus H for $p = 0.2$ and $\alpha = -0.6$ at $T = 2.5$ (broken curve) and $T = 3.5$ (full curve). \times and \bullet , $T = 2.5$ using AF and F initial spin configurations, respectively; $+$ and \circ , $T = 3.5$, using AF and F, respectively.

system. The existence of a hysteresis, which is not due to insufficient equilibrium time and of discontinuities in internal energy and staggered magnetisation mean that the transition is first-order, otherwise it is second-order. There are, however, some difficulties in the distinction between first- and second-order transitions in the tricritical region due to the following reasons: (i) in the MC procedure physical quantities are time- and space-averaged so that discontinuities associated with first-order transitions may be washed away and the results show features similar to those of a continuous transition; (ii) the finite size effects may round-up a first-order transition so that small samples which are too small are not useful; (iii) in addition, the position of a first-order critical point may change drastically with increasing sample size as it has been observed in the AF FCC Ising model [13]. These difficulties in analysing MC data in first-order transitions have been thoroughly discussed by Challa and co-workers [14] and Binder and Landau [14] (for works on finite-size scaling of first-order transitions see references cited in these papers). In view of these problems, the phase diagram shown in this paper should be read qualitatively.

Before showing our MC results we now discuss the equilibrium time. When the dilution becomes important, the time needed for equilibrating the system increases considerably near the transition. In previous MC studies with NN interactions only [3, 10], equilibrium times of order 10^6 MCS/spin have been used. However it is not our purpose here to determine each critical point and its associated critical exponents with high accuracy. Our aim is to show that a cross-over from first- to second-order transition exists and to study its dependence on p and α . At most we used 4×10^4 MCS/spin, half of which have been discarded for equilibrating. We have verified in each run that there is no significant time-dependence of the physical quantities. However, the above simulation time is not enough when p becomes larger than 0.3. The study of the case $p > 0.3$ is left to future work.

We show in figure 1 the staggered magnetisation m_{st} versus H for $p = 0.2$ and $\alpha = -0.6$ at $T = 2.5$ and $T = 3.5$ as typical examples of first- and second-order transitions, respectively. The system equilibrium can be seen by observing that both AF and F initial spin configurations yield the same result above and below the transitions within statistical errors. No attempt has been made to determine the transition point to high accuracy by taking smaller intervals between successive values of H , since this is beyond the scope of this work. For a first-order transition we take arbitrarily the transition point at the middle of the hysteresis cycle. For a second-order transition, the transition point is taken at the point of inflexion of m_{st} . The hysteresis width may be a convenient measure of the degree of first-order character since it decreases monotonically when one goes towards

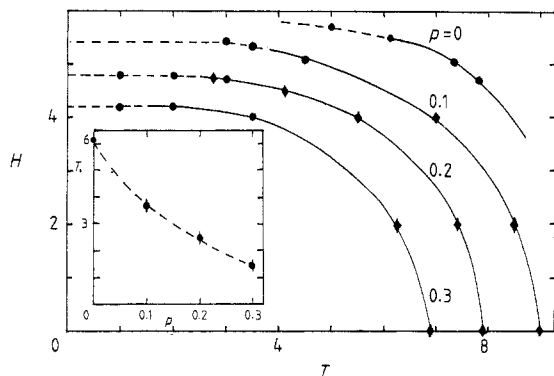


Figure 2. Phase diagram in the TH plane for $\alpha = -0.5$ at various values of p . \bullet , results of runs with fixed H ; \blacklozenge , results of runs with fixed T . First- and second-order critical lines are shown by broken and full curves, respectively. Results at $p = 0$ are taken from [15]. Inset: tricritical temperature as a function of p .

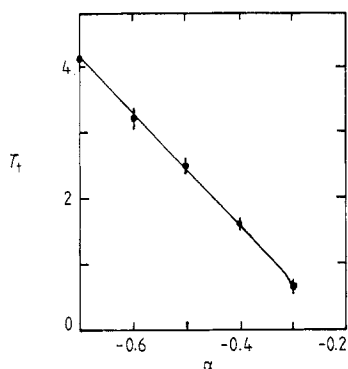


Figure 3. Tricritical temperature T_t versus α obtained by MC simulations. Vertical bars indicate errors. The full curve is a guide to the eye.

second-order regions in the TH plane. For a given p we look for the critical points at various values of H and T . In the first-order region we measure the hysteresis width and the tricritical point is taken where this width goes to zero by extrapolation. An example at $p = 0.2$ has been shown in [11]. The resulting phase diagram at $p = 0.1, 0.2$, and 0.3 for $\alpha = -0.5$ is shown in figure 2 where the results of Landau [15] for $p = 0$ are also presented. In the inset of figure 2, we show the tricritical temperature T_t as a function of p . It is observed that T_t decreases strongly with increasing p .

We note that at $p = 0.3$ the full AF order is often broken into domains of AF order. This is seen in runs with high temperature F initial spin configurations: below the transition the staggered magnetisation obtained upon cooling can be smaller than that obtained by heating from AF initial configurations. This effect is not due to metastability, since the local Edwards–Anderson order parameter in runs with F and AF initial conditions are identical within statistical errors.

We have also obtained the phase diagram in the $T\alpha$ plane for $p = 0.2$ shown in figure 3. The tricritical temperature T_t decreases linearly with increasing α . We could not accurately determine the value of α for which the tricritical point disappears. This is due to the well known difficulty with MC simulation at very low temperatures. We think however that this value is close to -0.2 (by extrapolation). Note that the critical value obtained from mean-field theory for the disappearance of the tricritical point in the non-dilute case [16] is $\alpha = -0.3$.

3. Probabilistic mean-field theory

To discuss the above results, we present a new mean-field calculation. A classical mean-field treatment of the Hamiltonian (1) with no dilution (i.e., $p = 0$) leads to the equation of state [16]

$$m = \sinh[2\beta(H - \delta m)] / \{ \cosh[2\beta(H - \delta m)] + \cosh[2\beta(H_s + \gamma m_s)] \} \quad (2)$$

and

$$m_s = \sinh[2\beta(H_s + \gamma m_s)] / \{ \cosh[2\beta(H - \delta m)] + \cosh[2\beta(H_s + \gamma m_s)] \} \quad (3)$$

where $\beta = 1/k_B T$, $m = (m_a + m_b)/2$, $m_s = (m_a - m_b)/2$, indices a and b denote the two sublattices of staggered symmetry, $\gamma = cJ + \alpha zJ$, $\delta = cJ - \alpha zJ$, c is the number of NN, z the number of NNN, and H_s a staggered field defined by $H_s = \partial g(T, H, m_s) / \partial m_s$ with the free energy given by

$$g(T, H, m_s) = g_0(T, H) + am_s^2 + bm_s^4 + cm_s^6 \quad (4)$$

with a , b , c being the Landau coefficients of an expansion in powers of the order parameter m_s .

We now present a probabilistic mean-field model. Since mean-field theory is a one-site approach, once dilution is introduced the various one-site configurations of the dilute problem should be included. There exist $7 \times 13 = 91$ configurations, depending on the respective numbers of both NN and NNN. We define these configurations through the variables $\gamma_{n,l}$ and $\delta_{n,l}$

$$\gamma_{n,l} = nJ + \alpha lJ \quad \delta_{n,l} = nJ - \alpha lJ \quad (5a)$$

with the probability

$$P_{n,l} = \frac{c!}{n!(c-n)!} \frac{z!}{l!(z-l)!} (1-p)^{n+l} p^{c+z-n-l}. \quad (5b)$$

The equations of state (2) and (3) become averages of equations of state over the various configurations (5). We obtain

$$m = \sum_{l=0}^z \sum_{n=0}^c P_{n,l} m(\beta, H, m, m_s, \gamma_{n,l}, \delta_{n,l}) \quad (6)$$

and

$$m_s = \sum_{n=0}^c \sum_{l=0}^z P_{n,l} m_s(\beta, H, m, m_s, \gamma_{n,l}, \delta_{n,l}). \quad (7)$$

It should be noted that $m_s(\beta, H, m, m_s, \gamma_{0,0}, \delta_{0,0}) = 0$ due to the staggered symmetry of the problem. From equation (7) the Curie temperature at $H = 0$ is found to be $\beta_C = (p\gamma)^{-1}$, which is the correct mean-field result. Expanding the above expressions in

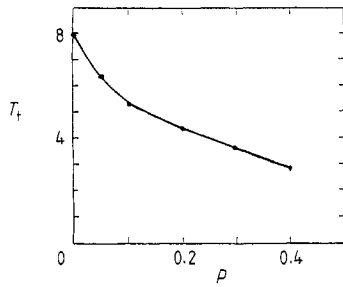


Figure 4. The tricritical temperature obtained by the probabilistic mean-field equations (8) and (9) as a function of p at $\alpha = -0.5$.

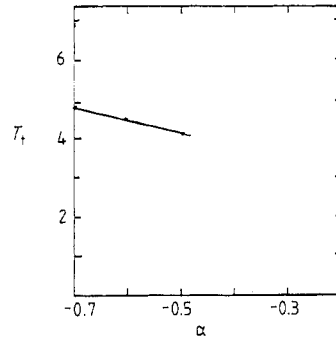


Figure 5. Mean-field tricritical temperature as a function of α at $p = 0.2$.

powers of m_s and using equation (4) we found a tricritical point when $a = b = 0$. The location of the tricritical point is given by

$$2\beta \sum_{n=0}^c \sum_{l=0}^z \frac{P_{n,l} \gamma_{n,l}}{1 + C_{n,l}} = 1 \tag{8}$$

and

$$\sum_{n=0}^c \sum_{l=0}^z \frac{P_{n,l}}{1 + C_{n,l}} \left(\frac{2}{3} \beta^3 \gamma_{n,l}^3 - \frac{2\beta^3 \gamma_{n,l}^3}{1 + C_{n,l}} + \frac{2\beta^2 \gamma_{n,l} \delta_{n,l} S_{n,l} m_2}{1 + C_{n,l}} \right) = 0 \tag{9}$$

where $C_{n,l} = \cosh[2\beta(H - \delta_{n,l} m_0)]$, $S_{n,l} = \sinh[2\beta(H - \delta_{n,l} m_0)]$,

$$m_0 = \sum_{n=0}^c \sum_{l=0}^z P_{n,l} \frac{S_{n,l}}{1 + C_{n,l}} \tag{10}$$

and

$$m_2 = -2\beta^2 \sum_{n=0}^c \sum_{l=0}^z \frac{P_{n,l} S_{n,l} \gamma_{n,l}^2}{(1 + C_{n,l})^2} \left/ \left[1 + 2\beta \sum_{n=0}^c \sum_{l=0}^z \frac{P_{n,l} \delta_{n,l}}{(1 + C_{n,l})^2} \left(C_{n,l} - \frac{S_{n,l}^2}{1 + C_{n,l}} \right) \right] \right. \tag{11}$$

The values of tricritical temperatures obtained from equations (8) and (9) are shown in figure 4 as a function of dilution p . Note the good qualitative agreement with MC results shown in the inset of figure 2. Figure 5 shows T_t as a function of α . The linear dependence of T_t on α is observed again here as in figure 3. Note, however, that for $\alpha \geq -0.4$ no solution of equations (8) and (9) is found and there is a discontinuity at $\alpha = -0.4$.

4. Conclusion

In conclusion we have shown that both NNN interactions and the dilution concentration can drastically change the phase diagram of the dilute Ising antiferromagnet in a magnetic field. Therefore, phase diagrams obtained in experiments for various systems may exhibit quite different features. For a given experiment, a tricritical point will thus either be expected or not expected depending on the actual values of both p and α . We have

also shown that results of MC simulations can be reproduced qualitatively by a very simple mean-field model.

Acknowledgments

The simulations have been carried out on the array processor FPS-164 of GRECO 'Expérimentation Numérique' at the Ecole Normale Supérieure, and partly on the super computer SX2 at NEC Corporation. One of us (HTD) is grateful to the NEC Corporation for its hospitality. Another (PA) is supported in this work by a contract granted by DRET (No 88/1331/DRET/DS/SR2).

We acknowledge fruitful comments by D Sherrington and J Villain on the mean-field part of this work.

References

- [1] Imbrie J 1984 *Phys. Rev. Lett.* **35** 1747
- [2] Imry Y and Ma S 1975 *Phys. Rev. Lett.* **35** 1399
- [3] Young A P and Nauenberg M 1985 *Phys. Rev. Lett.* **54** 2429
- [4] Galam S and Birman J L 1983 *Phys. Rev. B* **28** 5322
Andelman D 1983 *Phys. Rev. B* **27** 3079
Aharony A 1978 *Phys. Rev. B* **18** 3318
- [5] Fisher D S 1986 *Phys. Rev. Lett.* **56** 416
- [6] Fishman S and Aharony A 1979 *J. Phys. C: Solid State Phys.* **12** L729
- [7] Wong Pz, Von Molnar S and Dimon P 1982 *J. Appl. Phys.* **53** 7954; 1983 *Solid State Commun.* **48** 573
- [8] Belanger D P, King A R and Jaccarino V 1985 *Phys. Rev. B* **31** 4538
Yoshizawa H, Cowley R A, Shirane G and Birgeneau R J 1985 *Phys. Rev. B* **31** 4548
- [9] Villain J 1984 *Phys. Rev. Lett.* **52** 1547
Cambier J L and Nauenberg M 1986 *Phys. Rev. B* **34** 7998
- [10] Ogielski A T and Huse D A 1986 *Phys. Rev. Lett.* **56** 1298
- [11] Diep H T, Galam S and Azaria P 1987 *Europhys. Lett.* **4** 1068
- [12] Galam S 1987 *Phys. Lett. A* **121** 459
- [13] Pommier J, Diep H T, Ghazali A and Lallemand P 1988 *J. Appl. Phys.* **63** 3036
- [14] Challa M S, Landau D P and Binder K 1986 *Phys. Rev. B* **34** 1841
Binder K and Landau D P 1984 *Phys. Rev. B* **30** 1477
- [15] Landau D P 1976 *Phys. Rev. B* **14** 4054
- [16] Kincaid J M and Cohen E G D 1975 *Phys. Rept.* **22** 57